On the Transfer of Heat Generated by Energy Dissipation (Head Loss) to the Walls of Glacial Conduits: Revised Heat Transfer Coefficients

Aleah Sommers[1] and Harihar Rajaram[2]

[1]National Center for Atmospheric Research
[2]Johns Hopkins University

November 23, 2022

Abstract

The most general models for glacial hydrologic conduits include an energy equation, wherein a heat transfer coefficient controls the rate at which heat generated by mechanical energy dissipation is transferred to conduit walls, producing melt. Previous models employ heat transfer coefficients derived for engineering heat transfer problems, where heat is transferred between the walls of a conduit and a flowing fluid that enters the duct at a temperature different from the wall temperature. These heat transfer coefficients may not be appropriate for glacial hydrologic conduits in temperate ice, where the flowing fluid (water) and conduit walls (ice) are at almost the same temperature, and the heat generated by mechanical energy dissipation within the flow is transferred to the walls to produce melt. We revisit the energy transport equations that provide a basis for the derivation of heat transfer coefficients and highlight the distinctions between the heated walls and dissipated energy heat transfer cases. We present computational results for both cases across a range of Reynolds numbers in circular conduit and sheet geometries. For the heated walls case, our results are consistent with the widely used Dittus-Boelter heat transfer correlation, which has been used in previous glacial conduit models. We show that the heat transfer coefficient for transfer of heat generated by mechanical energy dissipation to conduit walls is smaller than that calculated using the Dittus-Boelter correlation by approximately a factor of 2.

On the Transfer of Heat Generated by Energy Dissipation (Head Loss) to the Walls of Glacial Conduits: Revised Heat Transfer Coefficients

A.N. Sommers[1,*], **H. Rajaram**[2,*]

[1]National Center for Atmospheric Research, Climate and Global Dynamics Laboratory
[2]Johns Hopkins University, Department of Environmental Health and Engineering
[*]Previously at University of Colorado, Department of Civil, Environmental, and Architectural Engineering

Key Points:

- New correlations are derived for heat transfer coefficients for transfer of dissipated mechanical energy as heat to walls of glacial conduits.
- Newly derived heat transfer coefficients are found to be lower than previously used coefficients based on heat transfer from heated walls, by a factor of two.
- Theoretical framework reproduces the classical Dittus-Boelter correlation for the heated wall case and clarifies why energy dissipation heat transfer is different.

Corresponding author: Aleah Sommers, aleahsommers@gmail.com

Abstract

The most general models for glacial hydrologic conduits include an energy equation, wherein a heat transfer coefficient controls the rate at which heat generated by mechanical energy dissipation is transferred to conduit walls, producing melt. Previous models employ heat transfer coefficients derived for engineering heat transfer problems, where heat is transferred between the walls of a conduit and a flowing fluid that enters the duct at a temperature different from the wall temperature. These heat transfer coefficients may not be appropriate for glacial hydrologic conduits in temperate ice, where the flowing fluid (water) and conduit walls (ice) are at almost the same temperature, and the heat generated by mechanical energy dissipation within the flow is transferred to the walls to produce melt. We revisit the energy transport equations that provide a basis for the derivation of heat transfer coefficients and highlight the distinctions between the heated walls and dissipated energy heat transfer cases. We present computational results for both cases across a range of Reynolds numbers in circular conduit and sheet geometries. For the heated walls case, our results are consistent with the widely used Dittus-Boelter heat transfer correlation, which has been used in previous glacial conduit models. We show that the heat transfer coefficient for transfer of heat generated by mechanical energy dissipation to conduit walls is smaller than that calculated using the Dittus-Boelter correlation by approximately a factor of 2.

Plain Language Summary

Most models of glacial hydrology that solve for the temperature of water and ice depend on heat transfer coefficients that are based on experiments of flow through pipes with heated walls. In and below glaciers, however, the ice walls are not heated but are almost the same temperature as the flowing water, and the commonly used correlations may not be appropriate. In this case, the flow itself produces heat through dissipation. We revisit the equations that heat transfer coefficients are based upon and highlight distinctions between these two situations. We present computational results of heat transfer coefficients for both cases. We find that heat transfer coefficients for the dissipation case are smaller than for the heated wall case by approximately a factor of 2.

1 Introduction

Heat transfer in laminar and turbulent shear flows is relevant to many engineering applications and in the context of geophysical flows. Heat transfer coefficients for various scenarios are well documented from theoretical and experimental studies (Kakaç et al., 1987; Incropera and DeWitt, 1996), and provide a basis for engineering design. Almost all previous heat transfer studies focus on heat transfer between the bulk fluid flow and conduit walls, either with constant wall temperature or a constant wall heat flux, and neglect the heat generated by dissipation of mechanical energy (commonly referred to as frictional or head loss). In most engineering and geophysical heat transfer scenarios involving air or water flows, this is a reasonable approximation. Notable exceptions arise in glaciology, however: Heat generated by mechanical energy dissipation (dominated by turbulent dissipation) in englacial and subglacial hydrologic flows is an important process in the dynamics of these systems (Röthlisberger, 1972; Nye, 1976; Spring and Hutter, 1981, Clarke, 2003). In englacial and subglacial hydrologic systems in temperate ice, both water and ice are typically near the melting point temperature, and the heat generated by mechanical energy dissipation is transferred to the walls, contributing to melting and enlargement of drainage conduit and sheet cross-sections. The important role of "strain heating" or the heat generated by viscous dissipation in the energy equation for ice sheets and glaciers is well established (Cuffey and Paterson, 2010).

The Nye (1976) model for outburst floods suggests a simplification of the general energy transport equation, assuming that all the heat generated by mechanical energy dissipation is locally and instantaneously transferred to the walls to produce melt enlargement. This approximation is employed in most subglacial hydrology models (e.g., Hewitt, 2011; Hewitt et al., 2012; Hewitt, 2013; Werder et al., 2013; Hoffman and Price, 2014; Sommers et al., 2018) and obviates the need for solving an energy transport equation, greatly facilitating computational tractability. However, in the case of outburst floods involving high advection velocities, some of the heat generated by mechanical energy dissipation can be advected downstream and the transfer of this heat to the walls is regulated by cross-sectional thermal diffusion. The Spring and Hutter (1981) and Clarke (2003) models employ a full energy equation, including a heat transfer coefficient that controls the rate at which heat generated by mechanical energy dissipation is transferred to the walls. Most previous models of outburst floods that include an energy equation typically parameterize this heat transfer coefficient by invoking the Dittus-Boelter correlation for the Nusselt number, which is a non-dimensional representation of the heat transfer coefficient (e.g., Nye, 1976; Spring and Hutter, 1981; Clarke, 2003; Creyts and Clarke, 2010). The Dittus-Boelter and comparable correlations for the Nusselt number (see Kakaç et al., 1987 for a comprehensive summary) are founded on the large body of research on engineering heat transfer, which considers the transfer of heat to/from a flowing fluid from/to the conduit walls, which are maintained at a different temperature. Clarke (2003) acknowledged that these correlations are not necessarily appropriate for representing the transfer of heat generated by mechanical energy dissipation to the walls of subglacial and englacial conduits, and suggested that this problem warranted further study. We are not aware of any previous studies that have explored this issue in detail.

The main goal of this paper is to evaluate the appropriateness of the Dittus-Boelter and related correlations for the transfer of heat generated by mechanical energy dissipation to the walls of englacial and subglacial conduits and sheets. We begin from the fundamental heat transport equations that provide a basis for the development of Nusselt number correlations for ducts/conduits (e.g. Incropera et al., 2007) and develop a computational framework for deriving these correlations in both laminar and turbulent flows. We consider both the classical heated wall heat transfer problem (we will refer to this problem as "heated wall case" for simplicity) and the transfer of heat generated by mechanical energy dissipation (which we will refer to as "dissipation case"), and highlight differences between these situations. See Figure 1 for a conceptual illustration of the two heat transfer cases. For turbulent flows, we employ previously verified representations for cross-sectional profiles of mean (time-averaged) velocity, eddy thermal diffusivity, and the turbulent dissipation rate. For the classical heated wall case, our computational results for the Nusselt number reproduce the Dittus-Boelter correlation. We show that the Nusselt numbers appropriate for the dissipation case are different from those for the heated wall case, and propose new correlations for the fully developed region.

2 Theoretical framework

2.1 Heat transport equations

Heat transfer coefficients for duct flows are derived from experimental studies and theoretical analyses based on the boundary layer approximations to the full energy trans-

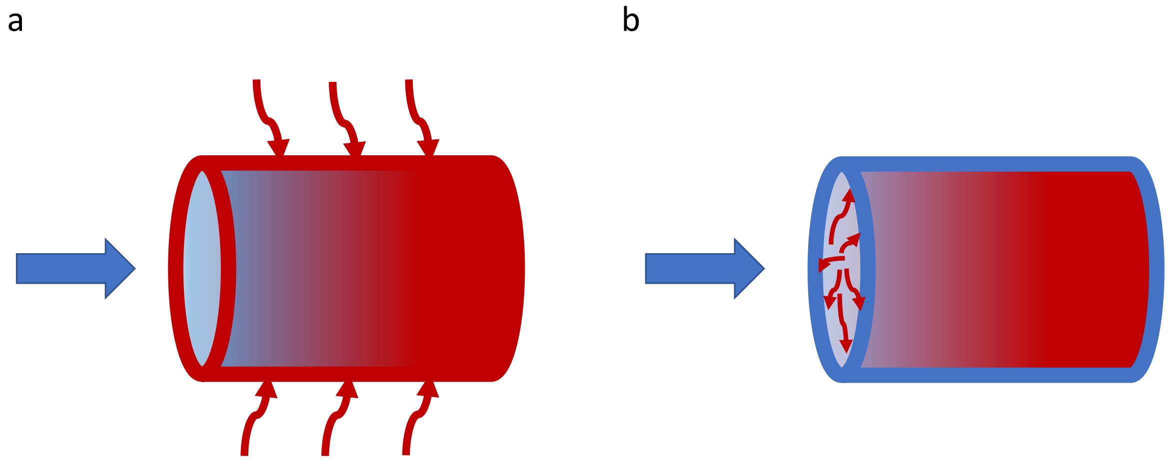

Figure 1. Two heat transfer scenarios are considered in this study: a) Heated wall case, in which water enters at a cooler temperature than the walls and is gradually heated downstream, and b) Dissipation case, in which water enters at the same temperature as the walls, and is heated by dissipation of mechanical energy within the flow.

port equation, which neglect axial conduction (Incropera et al., 2007). The general steady-state boundary layer approximations to the thermal energy equation in a circular conduit and two-dimensional sheet (geometries shown in Fig. 2) are:

Circular conduit flow:

$$u(r)\frac{\partial T}{\partial x} - \frac{1}{r}\frac{\partial}{\partial r}\left[r\left(\kappa + \kappa_T\right)\frac{\partial T}{\partial r}\right] = \frac{\Phi(r)}{\rho c_p} \tag{1}$$

Sheet flow:

$$u(z)\frac{\partial T}{\partial x} - \frac{\partial}{\partial z}\left[\left(\kappa + \kappa_T\right)\frac{\partial T}{\partial z}\right] = \frac{\Phi(z)}{\rho c_p} \tag{2}$$

In (1) and (2), u is the (time-averaged) mean streamwise velocity, T is the water temperature, x is the streamwise coordinate, κ is the molecular thermal diffusivity, κ_T is the turbulent eddy thermal diffusivity (κ_T=0 for laminar flow), r is a radial coordinate for circular conduit flow, z is a coordinate normal to the walls in sheet flow (with origin at the center), Φ is the mechanical energy dissipation rate, which represents the rate at which mechanical energy is converted to thermal energy, ρ is the fluid density and c_p is the specific heat of the fluid. In both laminar and turbulent flows, u and Φ vary across the cross-section of the flow as described below, while κ_T varies across the cross-

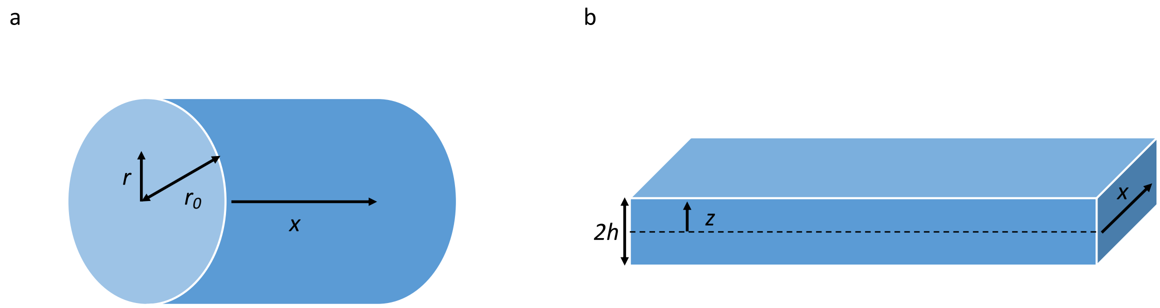

Figure 2. Schematic of geometries for a) Circular conduit, and b) Sheet flow.

section in turbulent flow and is zero in laminar flow. In the classical heated wall case, thermal energy resulting from mechanical energy dissipation is neglected (i.e. Φ=0), because it is very small in comparison to thermal fluxes between the wall and fluid driven by significant temperature differences. For laminar flows, heat transfer coefficients are derived by comparison of the solution to (1) or (2) with cross-section integrated heat transport equations. In a thermal entry region, the heat transfer coefficients vary along the axial direction, approaching a constant (fully developed) value corresponding to the smallest eigenvalue in the analytical solutions of (1) and (2) (Incropera et al. 2007, Shah and London, 1978). In turbulent flows, the velocity profiles and cross-sectional variation of eddy thermal diffusivity preclude analytical solutions, and numerical solutions or experimental studies have been used to derive heat transfer coefficients.

Although (1) and (2) are steady-state equations, the heat transfer coefficients derived from them are applicable to transient heat transfer problems involving time-varying entrance or wall temperatures, and to glacial conduits with evolving geometries. For example, the Spring-Hutter and Clarke equations (Spring and Hutter, 1981; Clarke, 2003) employ heat transfer coefficients that depend on the evolving conduit geometry and transient flow rates. This is justified by recognizing a time scale separation between the relatively slowly evolving axial temperature distributions along long conduits and the relatively rapid cross-sectional heat transfer processes that are represented using heat transfer coefficients.

2.2 Velocity profiles

For laminar flow, the velocity profile is the well-known parabolic profile described by:

Circular conduit flow:

$$u = 2u_b \left(1 - \frac{r^2}{r_0^2}\right) \tag{3}$$

Sheet flow:

$$u = \frac{3}{2}u_b \left(1 - \frac{z^2}{h^2}\right) \tag{4}$$

where u_b is the cross-sectional average velocity, r_0 is the radius of the circular conduit, and h is the half-depth of the sheet (the sheet extends from $z = -h$ to $+h$). For fully developed turbulent flow, several alternative descriptions of the (time-averaged) mean velocity profile are available in the literature. These descriptions typically involve different expressions in the viscous sublayer, a buffer region and an inner turbulent core where the log-law velocity profile is valid.

We employ the following dimensionless velocity profiles for $u^+ = u/u_\tau$, where u_τ is the shear velocity and $z^+ = (h-|z|))u_\tau/\nu$ is the wall coordinate for sheet flow, which is replaced by $z^+ = (r_0 - r)u_\tau/\nu$ for circular conduit flow:

$$u^+ = \frac{1}{K} \ln z^+ + B, \quad z^+ > 20 \tag{5}$$

$$u^+ = z^+ + \beta_1 z^{+4} + \beta_2 z^{+5}, \quad z^+ \leq 20 \tag{6}$$

Equation (5) is the familiar log-law velocity profile, while equation (6) for the wall region is adapted from (Wasan et al., 1963) with the constants $\beta_1 = -1.2533 \times 10^{-4}$ and $\beta_2 = 3.9196 \times 10^{-6}$ to allow for a smooth transition with matching derivatives in the velocity profile between the log-law region and the viscous sublayer where $u^+ \approx z^+$. Equation (6) also ensures that the eddy viscosity is continuous and vanishes near the wall with a cubic dependence on distance from the wall (Townsend, 1976; Tien and Wasan, 1963). Figure 3 shows illustrative non-dimensional velocity profiles for different Reynolds numbers (Re=$u_b(2h)/\nu$ or $u_b(2r_0)/\nu$ for the sheet or circular conduit respectively).

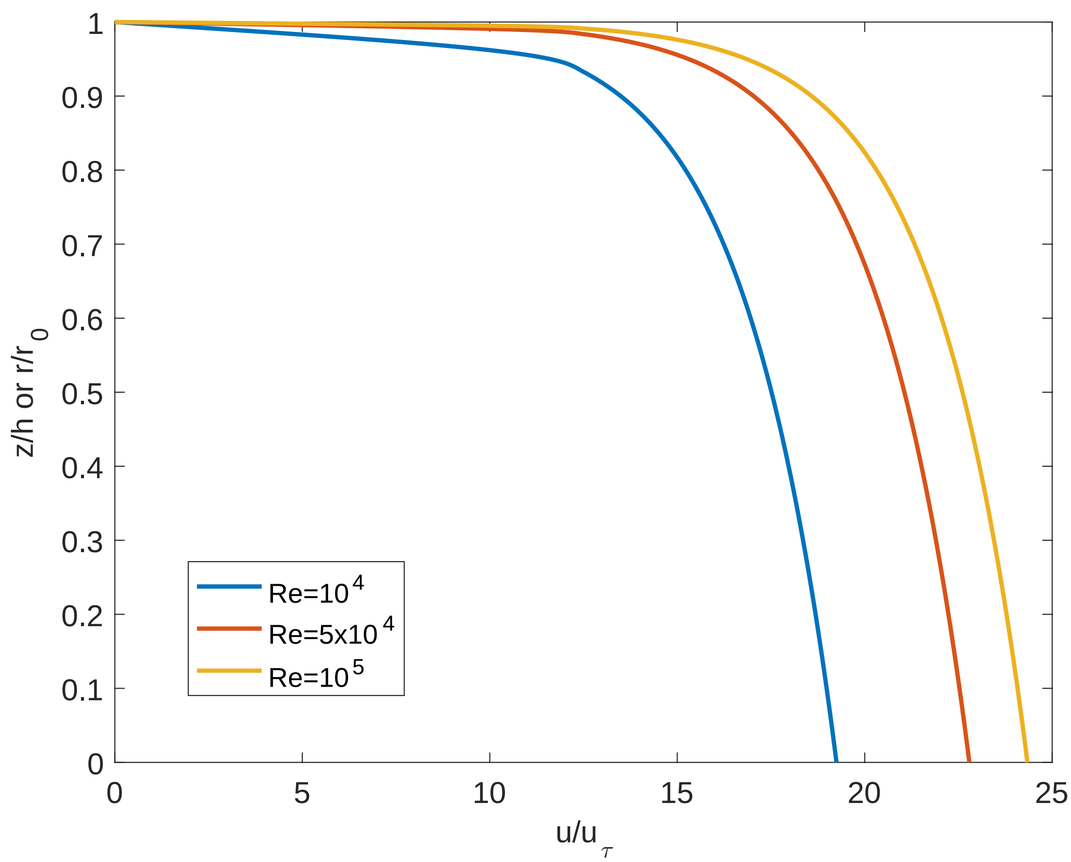

Figure 3. Fully developed turbulent velocity profile (used for both circular conduit and sheet).

2.3 Eddy viscosity and thermal diffusivity

The eddy viscosity (ν_T) profile is obtained directly from the mean velocity profile defined above, based on its fundamental definition in terms of the total shear stress (τ):

Circular conduit:

$$\tau = -\rho(\nu + \nu_T)\frac{\partial u}{\partial r} \tag{7}$$

Sheet:

$$\tau = -\rho(\nu + \nu_T)\frac{\partial u}{\partial z} \tag{8}$$

The shear stress varies linearly from zero at the center of a circular conduit or sheet flow to a maximum value at the walls, τ_w (wall shear stress), i.e.

Circular conduit:

$$\tau = \tau_w \frac{r}{r_0} \tag{9}$$

Sheet:

$$\tau = \tau_w \frac{z}{h} \tag{10}$$

The eddy thermal diffusivity is obtained from Reynolds analogy (Bird et al., 1960):

$$\kappa_T = \nu_T \tag{11}$$

Figure 4 shows profiles of κ_T/κ for different Reynolds numbers.

2.4 Wall shear stress and skin friction

For fully developed steady flow, the wall shear stress is related to the hydraulic gradient:

Circular conduit:

$$\tau_w = -\frac{\partial}{\partial x}(p + \rho g z_e)\frac{r_0}{2} \tag{12}$$

Sheet:

$$\tau_w = -\frac{\partial}{\partial x}(p + \rho g z_e)h \tag{13}$$

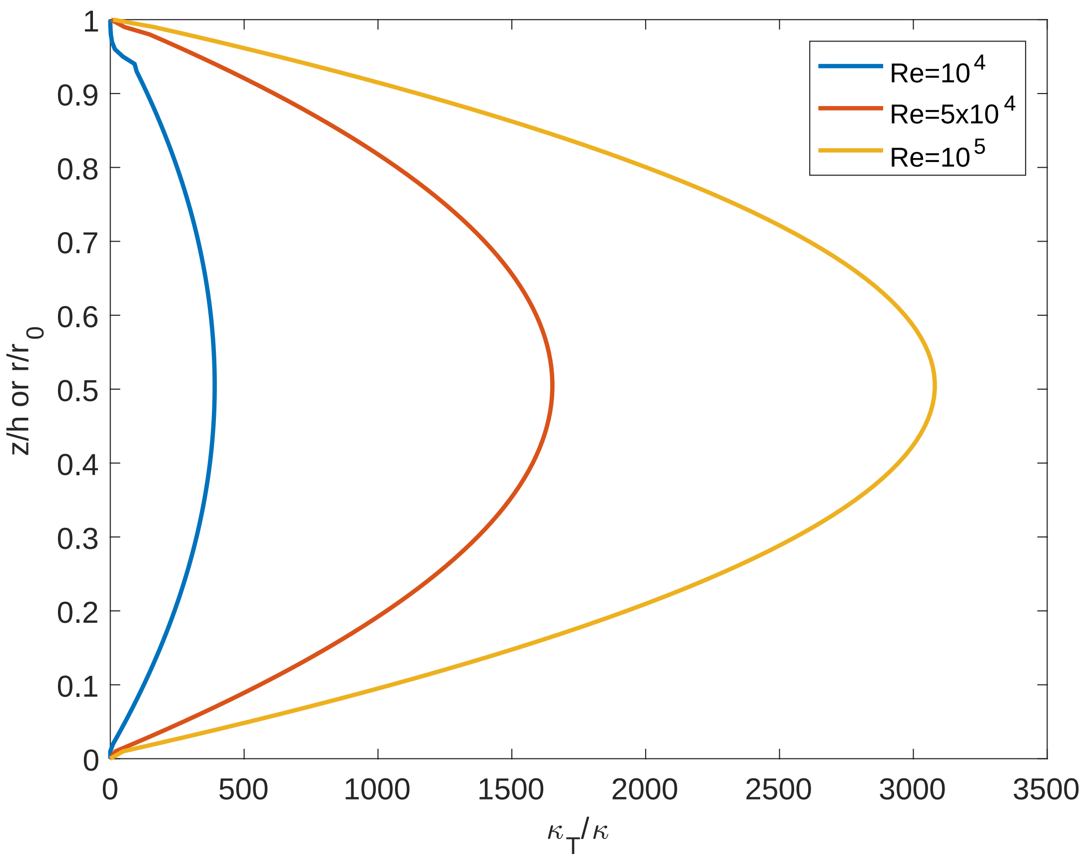

Figure 4. Turbulent (eddy) thermal diffusivity profile.

where z_e is the vertical elevation of the conduit or sheet, to account for non-horizontal alignment. The wall shear stress is also related to the Darcy-Weisbach friction factor (f) by:

$$\tau_w = \frac{1}{8} f \rho u_b^2 \tag{14}$$

The Darcy-Weisbach friction factor f is related to the skin friction factor $C_f = f/4$, and can be found by solving the following relation (Zanoun et al., 2009):

$$2\sqrt{\frac{2}{f}} = \frac{1}{\kappa} \ln\left(\frac{Re}{4}\sqrt{\frac{f}{2}}\right) - \frac{1}{\kappa} + B \tag{15}$$

The shear velocity u_τ used to non-dimensionalize the velocity profiles and define the wall coordinate is related to the wall shear stress by the well-known relationship $u_\tau = \sqrt{\tau_w/\rho}$.

2.5 Energy dissipation rate profile

The general thermal energy equation for incompressible fluid flow includes a source term that represents heat generated from the dissipation of mechanical energy by work done against shear forces. As noted above, this term is typically negligible in engineering heat transfer problems. In incompressible turbulent conduit or sheet flow, the (time-averaged) mean mechanical energy dissipation rate per unit volume (Φ) includes both viscous dissipation associated with the mean flow and dissipation of turbulent kinetic energy (turbulent dissipation). The latter is produced from the work done by the mean flow against turbulent (Reynolds) stresses, and eventually dissipated by viscosity into thermal energy (Hinze, 1975). In fully developed turbulent flows in conduits, the cross-sectional integrals of turbulent kinetic energy production and dissipation are equal, even though their profiles are different (Hinze, 1975; Laadhari, 2007). The total dissipation rate Φ is given by:

$$\Phi = \Phi_{mean} + \Phi_T = \rho\left(\nu\left(\frac{\partial u}{\partial z}\right)^2 + \epsilon\right) \tag{16}$$

where the turbulent dissipation rate ϵ is defined from the turbulent part of the velocity deformation tensor as (Laadhari, 2007):

$$\epsilon = \nu \left(\overline{\frac{\partial u_i'}{\partial x_j} \frac{\partial u_i'}{\partial x_j}} + \frac{\partial^2 \overline{u_i' u_j'}}{\partial x_i \partial x_j} \right) \tag{17}$$

In (17), the primed quantities denote turbulent velocity fluctuations and the overbar denotes a time average. The variation of the viscous dissipation term (first term in Eq. 16) across the flow cross-section is readily calculated from the mean velocity profile defined in Eqs. (5) and (6) above. The cross-sectional profiles of the turbulent dissipation rate, ϵ, need to be parameterized based on data from experiments or direct numerical simulations (DNS). Some of the first experimental and theoretical efforts to characterize the cross-sectional profile of the turbulent dissipation term were conducted by Taylor (1935). Subsequently, the cross-sectional profile of ϵ has been discussed in several works (e.g., Rotta, 1962; Lawn, 1971; Kock and Herwig, 2003; Laadhari, 2007). We prescribe the dissipation profile following the recent work of Abe and Antonia (2016), which is based on a synthesis of several contemporary DNS studies. For sheet flow, we adopt the correlations presented by Abe and Antonia (2016) for the dimensionless turbulent dissipation rate:

$$\frac{\epsilon h}{u_\tau^3} = \frac{2.45}{\left(1 - \frac{|z|}{h}\right)} - 1.7, \quad \left(1 - \frac{|z|}{h}\right) > 0.2 \tag{18}$$

$$\frac{\epsilon h}{u_\tau^3} = \frac{2.54}{\left(1 - \frac{|z|}{h}\right)} - 2.6, \quad \left(1 - \frac{|z|}{h}\right) \leq 0.2, \quad z^+ > 30 \tag{19}$$

$$\frac{\epsilon h}{u_\tau^3} = \frac{2.54}{\left(\frac{30}{h^+}\right)} - 2.6, \quad z^+ \leq 30 \tag{20}$$

The corresponding expressions for circular conduit flow are readily obtained readily by replacing $|z|/h$ with r/r_0 (Abe and Antonia, 2016). Note that very near the wall ($z^+ \leq 30$), the dissipation rate is a constant, equal to the value obtained from Eq. (19) at $z^+ = 30$. This behavior is consistent with the profiles of $\epsilon h/u_\tau^3$ presented by Abe and Antonia (2016). Figure 5 shows the turbulent and viscous dissipation profiles in fully developed turbulent flow. Although viscous dissipation is predominant near the wall, turbulent dissipation dominates through the bulk of the fluid profile.

For fully developed flows, the integral of the total mechanical energy dissipation rate over the flow cross-section should be equal to the power input to the system by the

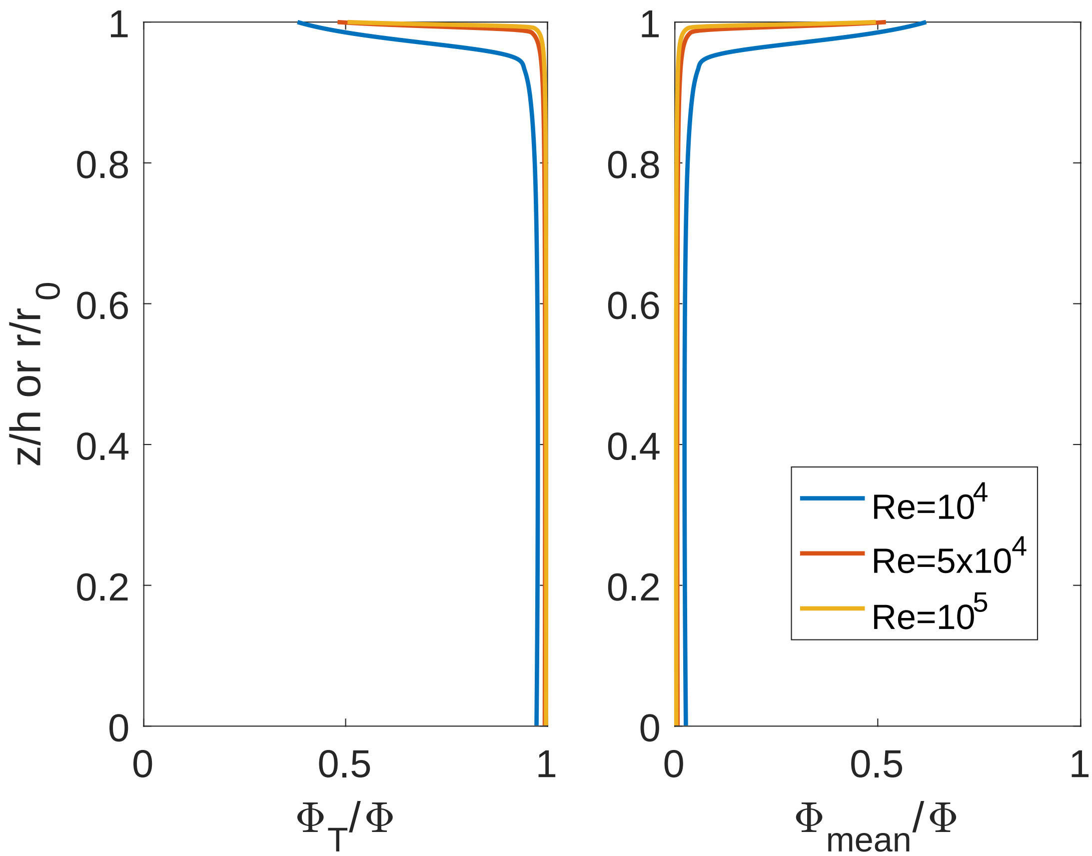

Figure 5. Turbulent dissipation (left) and viscous dissipation profiles (right) for various Reynolds numbers in fully developed turbulent flow (normalized by the total dissipation). Turbulent dissipation is most important through the bulk of the fluid, but viscous dissipation dominates close to the wall.

mean pressure (or more generally pressure and gravitational) gradient. For sheet flow, this implies that $E = u_\tau^2 u_b = \langle\Phi\rangle/2\rho$ (Abe and Antonia, 2016), where $\langle\Phi\rangle$ denotes the integral of Φ across the sheet depth (i.e. –h to +h). In Figure 6, we compare $\langle\Phi\rangle/2\rho$ obtained by numerically integrating the total dissipation profile of Φ from (16) and (18)-(20) over half the channel width, with the corresponding theoretical value of $u_\tau^2 u_b$, confirming the consistency of our representation of the dissipation function across a range of Reynolds number values. For the sheet, note that ρE and $\langle\Phi\rangle$ have units of W/m^2 (rate of mechanical energy loss per unit width in the third dimension, per unit length along the flow direction). In the case of the circular conduit, $2\pi r_0 \rho E$ and $\langle\Phi\rangle$ have units of W m^{-1} (representing the rate of mechanical energy loss per unit length along the flow direction).

2.6 Estimation of Nusselt numbers from numerical solutions of the heat equation

The heat transfer coefficient H is defined based on the cross-section integrated heat transport equation over the conduit area or across the sheet width. For the circular conduit, the cross-section integrated equation is of the form:

$$\rho c_p Q \frac{dT_b}{dx} = \langle\Phi\rangle + 2\pi r_0 H (T_w - T_b) \tag{21}$$

where Q is the flow rate through the pipe ($Q = \pi r_0^2 u_b$ for the circular conduit), $\langle\Phi\rangle$ is the dissipation rate integrated over the cross-sectional area of the pipe, T_w is the wall temperature, and T_b is the flux-averaged bulk fluid temperature (i.e. mixing cup temperature, Incropera et al., 2007). Angular brackets indicate integration over the flow cross-section. In sheet flow, the depth-integrated heat transport equation accounts for the heat flux to both walls:

$$\rho c_p q \frac{dT_b}{dx} = \langle\Phi\rangle + 2H (T_w - T_b) \tag{22}$$

where $q = u_b(2h)$ is the flow rate per unit width (in the third dimension) in the sheet. As noted earlier, $\langle\Phi\rangle$ has different units in the circular conduit (W m^{-1}) and sheet (W m^{-2}) geometries.

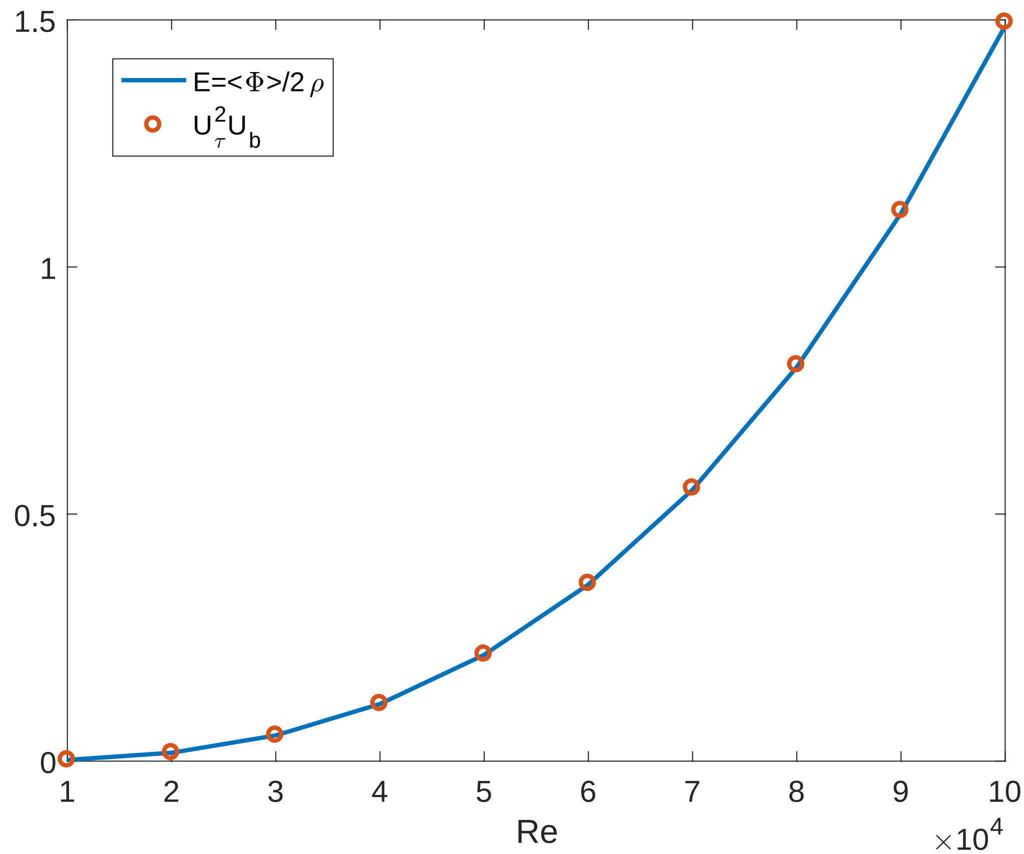

Figure 6. A comparison of the integral of the scaled dissipation rate $\langle\Phi\rangle/2\rho$ obtained by numerical integration of (16) with (18)-(20) for the turbulent dissipation rate ϵ over half the sheet depth, with the corresponding theoretical value of $E = u_\tau^2 u_b$, across a range of Reynolds numbers.

As noted previously, heat transfer coefficients implied by (1, 2) and (21, 22) are applicable to transient heat transfer problems involving time-varying entrance or wall temperatures, based on a time scale separation between the slowly evolving axial temperature distributions along and the relatively rapid cross-sectional heat transfer processes. In general, the heat transfer coefficients in (21) and (22) also depend on x in a thermal entry region before a fully developed temperature profile is attained and H approaches a constant value. The heat transfer coefficient is generally larger than its asymptotic constant value in the thermal entry region, whose length is a complex function of Reynolds and Prandtl numbers, and is generally around 20-30 times the conduit diameter in circular conduits (Kays and Crawford, 1993). In typical applications to long conduits (including previous applications to glacial conduits), fully developed values of the heat transfer coefficient are used to represent heat transfer, because the entry length is considered to be a relatively small fraction of the overall conduit length. We will therefore focus on estimating the fully developed values of the heat transfer coefficient (or equivalently Nusselt number).

Heat transfer coefficients are typically represented in dimensionless form based on the Nusselt number:

$$Nu = \frac{HL}{k} \tag{23}$$

where H is the heat transfer coefficient, L is a characteristic length, and k is the thermal conductivity of the fluid ($k = \rho c_p \kappa$). The characteristic length commonly used in the definition of Nu is $L = 4P/A$, where P is the perimeter and A is the cross-sectional area (Shah and London, 1978; Incropera et al., 2007). For a circular conduit, $L = 2r_0$ (i.e. the pipe diameter). For a wide, flat sheet, $L = 4h$ (i.e. twice the sheet width).

As noted in Section (2.1) above, the fully developed heat transfer coefficient or Nusselt number for various heat transfer problems can be estimated by comparing the cross-sectional averages of the numerical (or analytical in some cases) solutions of (1) or (2) with the analytical solutions of (21) or (22), beyond the thermal entry length, where $H(Nu)$ has attained a constant value. We solved (1) and (2) numerically for the circular conduit and sheet cases respectively, to estimate Nusselt numbers. For turbulent flow regimes, we estimated Nusselt numbers over a range of Reynolds numbers.

The thermal energy equations (1) and (2) are parabolic, with the coordinate x along the flow direction playing the role of a time-like variable. We solved these equations numerically using a finite-difference discretization in the cross-flow direction (z or r), and an implicit Crank-Nicholson scheme along x. Due to the sharp variations of the mean velocity, eddy thermal diffusivity and dissipation function in the vicinity of the walls, especially at higher Reynolds numbers, we used very fine discretization along z (or r). We carried out grid sensitivity studies to verify that all the computational results reported below had converged and were insensitive to additional grid refinement.

We estimated Nusselt numbers for two distinct cases – the heated wall case and the dissipation case (Fig. 1). We considered the heated wall case (neglecting dissipation, $\Phi = 0$) to verify that our computational framework and assumed profiles for various quantities (Sections 2.2-2.4) consistently reproduce previously well-established theoretical and empirical correlations for Nusselt numbers. In the heated wall case, the boundary condition for fluid temperature on the walls was assigned as $T = T_w$ (at $r = r_0$ in the circular conduit geometry and $z = \pm h$ in the sheet geometry). For the circular conduit geometry, a symmetry boundary condition ($\partial T/\partial r = 0$) was assigned at the center ($r = 0$). At the entrance ($x = 0$), the fluid temperature across the entire cross-section was set to $T = T_0$. We used values of $T_w = 1$ and $T_0 = 0$ for convenience. With $\langle\Phi\rangle = 0$, the solutions of (21) and (22) suggest that $(T_w - T_b)$ will decrease exponentially along the conduit axis (equivalently, $\ln(T_w - T_b)$ will decrease linearly) in the thermally fully developed region where H (Nu) has attained a constant value (Shah and London, 1978). The numerical solution of T_w obtained from (1) or (2) can be used to calculate the variation of T_b along x. The corresponding $\ln(T_w - T_b)$ estimate will exhibit a faster decrease near the entrance, and transition to a linear decrease in the thermally fully developed region. The heat transfer coefficient H (and thus Nu) can be estimated from the slope (m) of a linear fit to the variation of $\ln(T_w - T_b)$ with x. More details are given in Appendix 1.

In the dissipation case, the complete dissipation rate profile (Section 2.5) is included in the numerical solution of (1) and (2). The boundary condition for fluid temperature on the walls (T_w) was assigned equal to the fluid temperature (T_0) at the entrance (in the case of glacial conduits in temperate ice, both these temperatures are equal to the melting point temperature). In this case, the fluid is warmed by the heat generated from dissipated mechanical energy and transfers heat to the walls. In glacial conduits in temperate ice, the heat transferred to the walls produces melt. At some downstream distance from the entrance, a fully developed temperature profile will be attained that remains invariant along x thereafter, corresponding to which $dT_b/dx = 0$. In this fully thermally developed region, there is a balance between heat generated by mechanical energy dissipation and heat transfer to the walls. The heat transfer coefficient H (and thus Nu) can be estimated by calculating the fully developed bulk temperature from the numerical solutions of (1) and (2). More details are given in Appendix 1.

3 Results

3.1 Laminar flow

Figure 7 shows temperature profiles at different distances from the conduit entrance in laminar flow for the wall heat transfer and dissipation cases, and illustrates the phenomenology noted in Section 2.6 above. For the heated wall case in laminar flow with $\Phi = 0$, the Nusselt numbers for the circular pipe and sheet cases are well known (Incropera et al. 1996) and equal to 3.66 and 7.54, respectively. Nusselt numbers calculated based on our numerical solutions to (1) and (2) and the approach described in Section 2.6 and Appendix 1, matched these theoretical values.

Using the approach described in Section 2.6 for the dissipation case, the Nusselt numbers for transfer of dissipated mechanical energy to the walls were determined to be 2.40 and 4.99 for the circular conduit and sheet respectively. These values are smaller than the corresponding Nusselt numbers for the heated wall case.

3.2 Turbulent flow

Figure 8 shows a typical set of temperature profiles at different distances from the conduit entrance for fully developed turbulent flow, with $\mathrm{Re} = 10^4$ and a Prandlt number ($\mathrm{Pr} = \nu/\kappa$) = 13.5 (corresponding to water at 0 degrees C). To explore the dependence of the Nusselt number on Reynolds number, we performed numerical simulations of (1) and (2) for a range of Reynolds numbers. For each value of Reynolds number, the friction factor (f) was determined from (15) and used to calculate the wall shear stress and shear velocity, from which the velocity, eddy diffusivity and dissipation profiles were calculated. Nusselt numbers were estimated across a range of Re using the approach described in Section 2.6 and Appendix 1. Figures 9 and 10 respectively show the variation

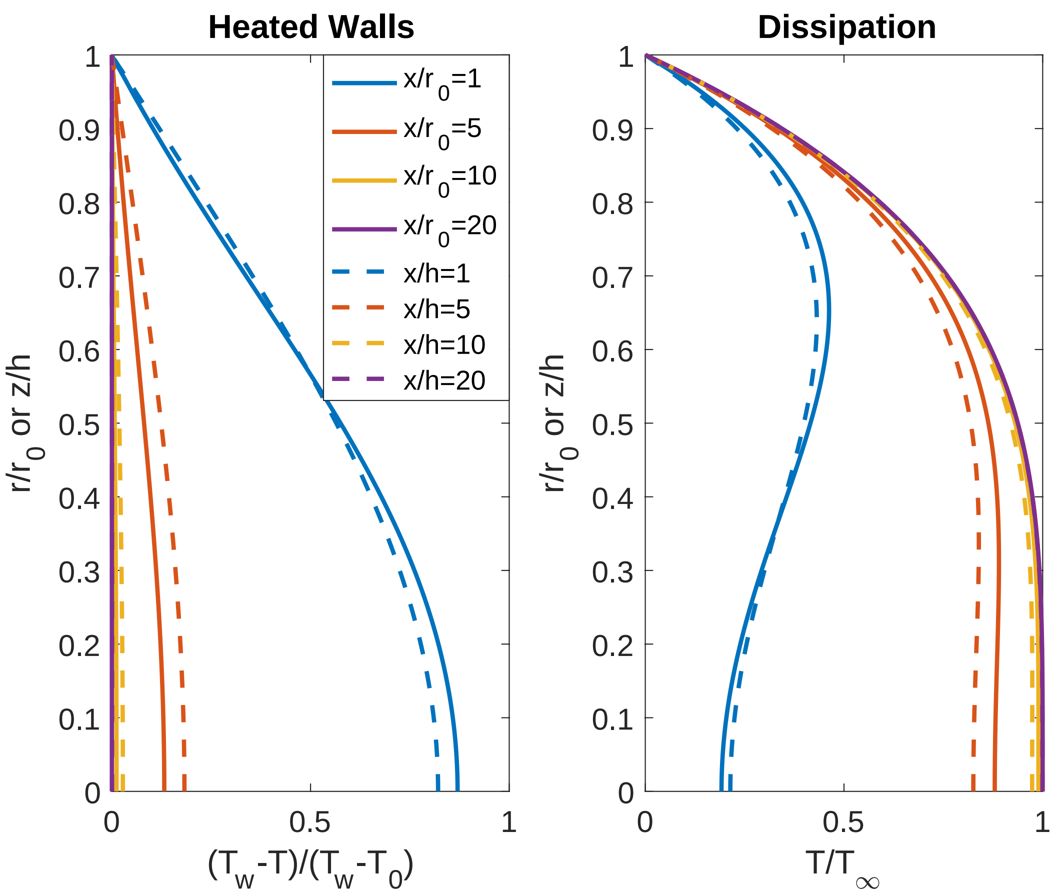

Figure 7. Temperature profile evolution for laminar flow through a circular conduit and flat sheet in the (a) heated wall and (b) internal dissipation cases. Note that T_∞ used to non-dimensionalize the temperature in the dissipation case is defined as the temperature at the flow center of the cross-section ($r = 0$ or $z = 0$) in the fully developed thermal region.

of Nusselt number with Reynolds number for the circular conduit and sheet flow geometries. For the circular conduit case, Figure 9 also shows the Nusselt number values obtained using the Dittus-Bolter correlation. The Dittus-Boelter correlation was developed for $0.7 \leq Pr \leq 120$ and $2500 \leq Re \leq 1.24 \times 10^5$. It is frequently used due to its simplicity:

$$Nu = 0.024 Re^{0.8} Pr^{0.4} \tag{24}$$

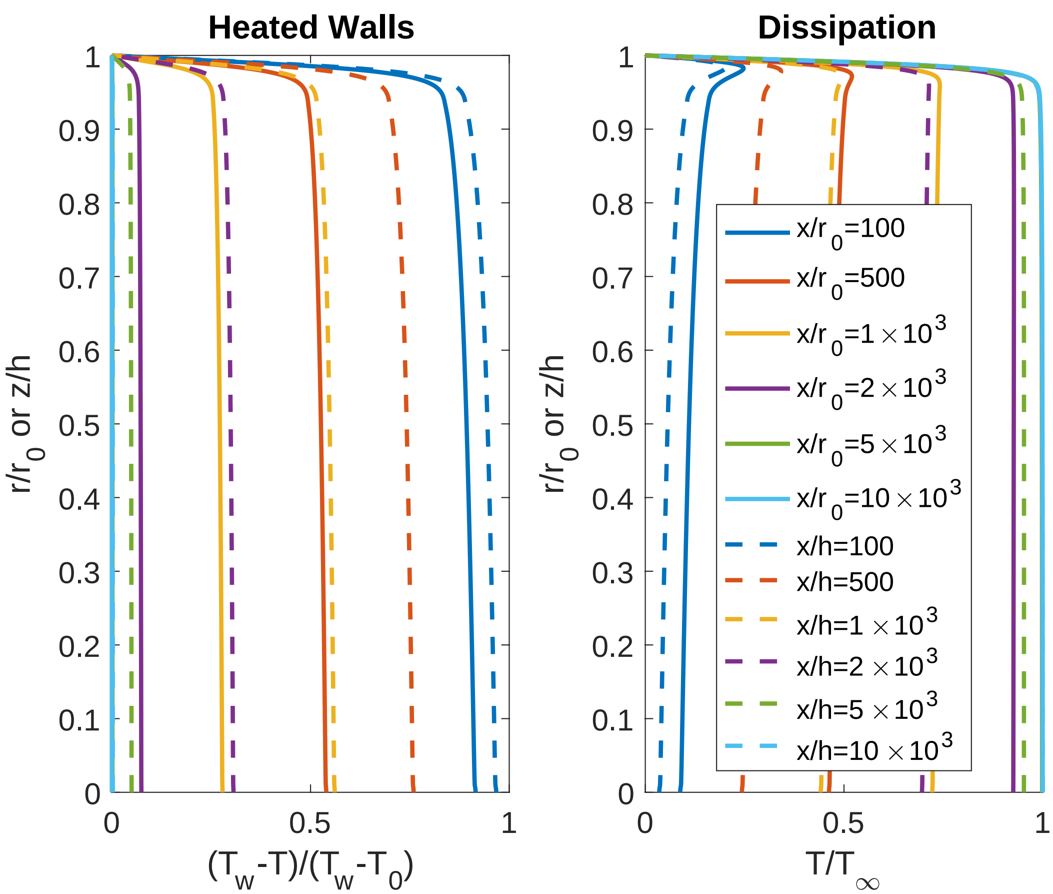

Figure 8. Temperature profile evolution for fully developed turbulent flow ($Pr = 13.5$, $Re = 10,000$) in the (a) heated wall and (b) internal dissipation cases. Temperature profiles are shown for both the circular conduit and sheet. Note that T_∞ used to non-dimensionalize the temperature in the internal dissipation case is defined as the temperature at the center of the cross-section (r=0 or z=0) in the thermally fully developed region.

For $3 \leq Pr \leq 10$ (typical values for water), the Dittus-Boelter correlation is 15% lower to 7% higher than the well respected Gnielinski correlation (Kakaç et al., 1987). For the circular conduit, our estimates of the Nusselt number for the heated wall case agree very well with values obtained using the Dittus-Boelter correlation (Figure 9), confirming that our overall approach accurately represents heat transfer processes for this previously well studied problem. Thus, our approach incorporating the dissipation function Φ from Section 2.5 is expected to accurately represent the transfer of heat generated by mechanical energy dissipation over the cross-section to the walls. For the circular conduit, the corresponding Nusselt number is smaller than that predicted by the Dittus-Boelter correlation by about a factor of 2 (Figure 9). Figure 10 shows the Nusselt number as a function of Reynolds number for fully developed turbulent flow in a wide sheet. The Nusselt number correlations for a circular pipe are also shown for comparison. As in circular conduit flow, the Nusselt number for the dissipation case is smaller than that for the heated wall case. The Nusselt numbers for the channel are systematically larger than in the circular conduit. Somewhat coincidentally, the Nusselt number for transfer of dissipated energy in the sheet is very close to the Nusselt number for the circular conduit heated wall case.

Our numerical simulation results and fitted values of Nusselt number suggest a power-function relationship between Nu and Re, of the form $Nu = a\mathrm{Re}^b\mathrm{Pr}^{0.4}$, where the 0.4 exponent for the Prandtl number is retained from the Dittus-Boelter correlation. Values of a and b were fit to the estimated Nusselt numbers, yielding the following Nusselt number correlations for the transfer of heat generated by mechanical energy dissipation in a circular conduit and wide sheet:

Circular conduit:

$$Nu = 0.0032Re^{0.9325}Pr^{0.4} \tag{25}$$

Sheet:

$$Nu = 0.0055Re^{0.9415}Pr^{0.4} \tag{26}$$

4 Conclusions

The motivation for this exploration was to examine in detail the suitability of heat transfer correlations commonly used in englacial and subglacial hydrology models. Specifically, we were inspired to determine whether heat transfer correlations developed for the

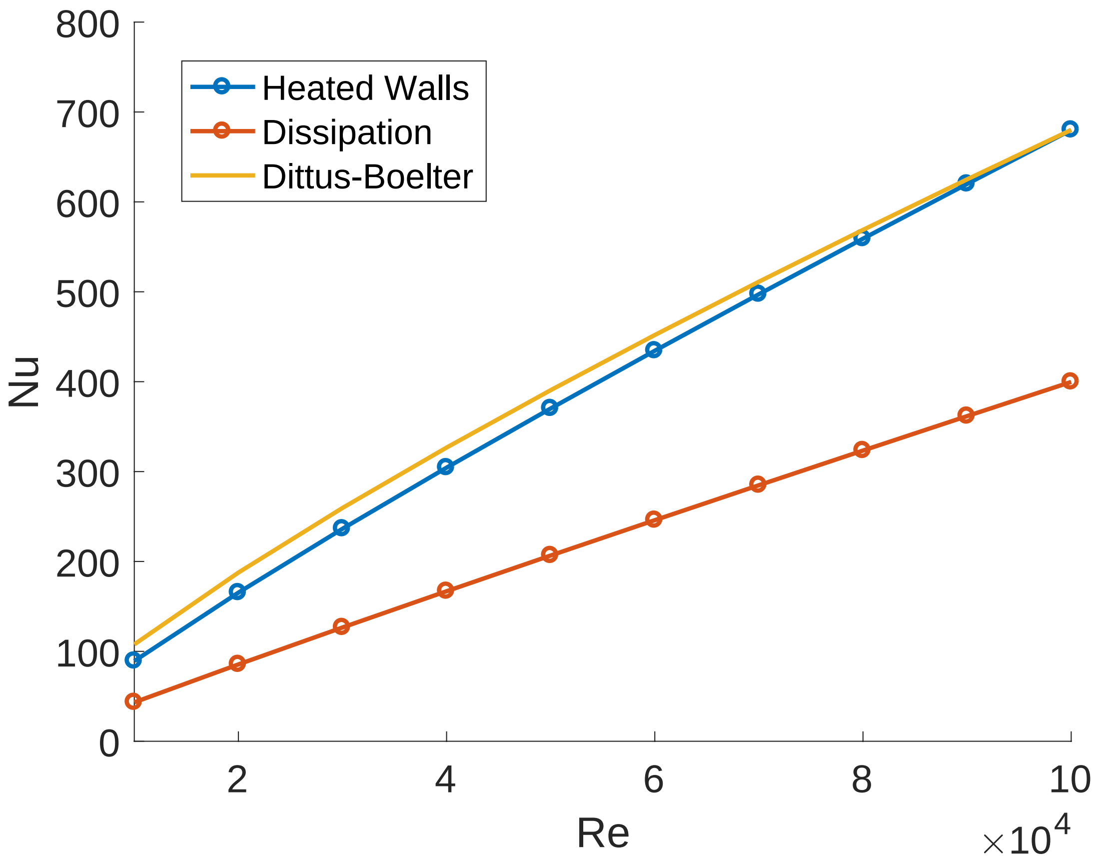

Figure 9. Nusselt number as a function of Reynolds number for fully developed turbulent flow with $Pr = 13.5$ through a circular conduit for the heated wall case and for the dissipation case, compared with empirical correlations for the heated wall case. For the dissipation case, Nu is consistently lower than in the heated wall case.

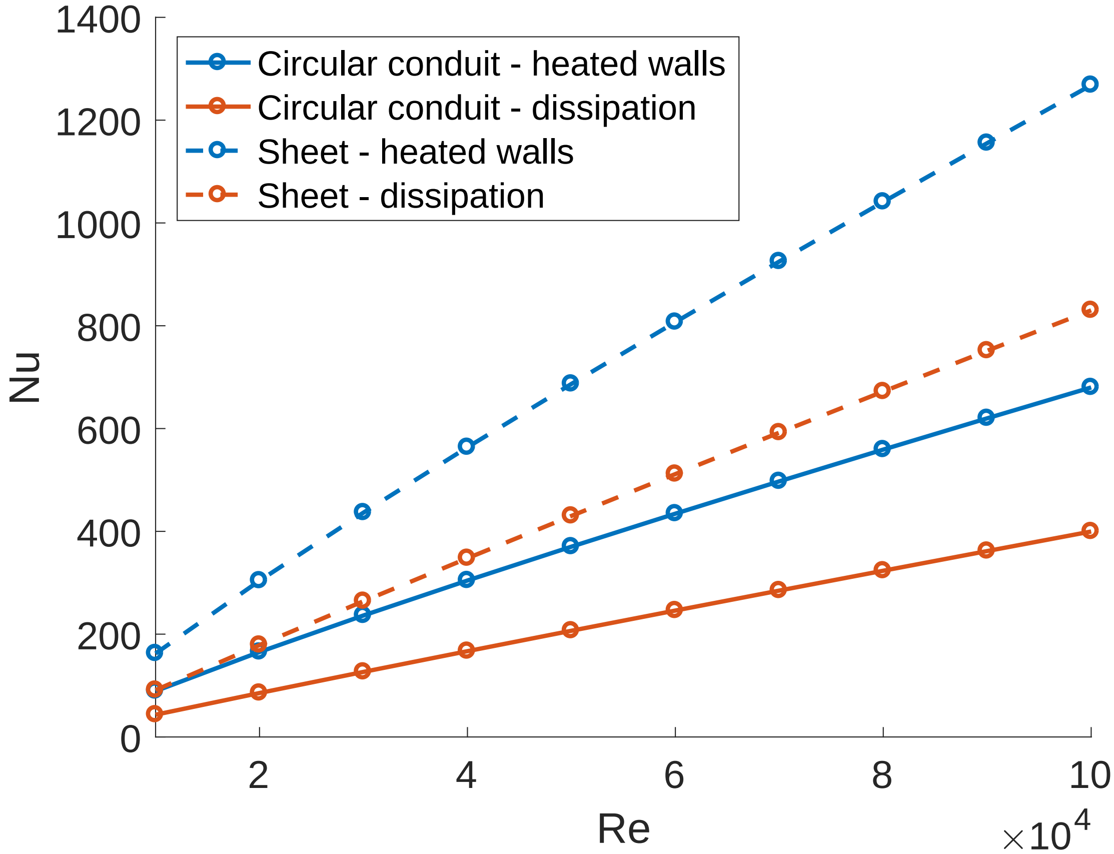

Figure 10. Nusselt number as a function of Reynolds number for fully developed turbulent flow with $Pr = 13.5$ through a sheet with heated walls and for the dissipation case. The corresponding Nusselt numbers for the circular conduit are shown for comparison. For both the circular conduit and the sheet, Nusselt numbers for the dissipation case are smaller than in the heated wall case.

wall heat transfer case with no internal dissipation would accurately represent heat transfer in a scenario where internal dissipation is the main source of heat. Our results show that Nusselt numbers corresponding to the dissipation case are consistently lower than those for the wall heat transfer case (Figs. 9 and 10) for both a circular conduit and a sheet. We determined correlations based on our numerical results for heat transfer from internal dissipation for fully developed turbulent flow through a circular conduit and a sheet in Eqs. (25) and (26), respectively. These correlations may be used in place of traditional wall heat transfer correlations in solving the energy equation in englacial or subglacial hydrology models for improved physical completeness and accuracy.

While the Nusselt number is consistently smaller with internal dissipation than with heated walls, the difference is only about a factor of two (not an order of magnitude difference). Even so, this small difference may have significant implications for how quickly a viable subglacial drainage system can form when liquid meltwater is introduced into cold ice, as melt increases further inland on ice sheets with warming air temperatures at higher elevations. We leave this problem open for further research.

Appendix A Appendix 1

In the heated wall case with $\langle \Phi \rangle = 0$, (21) and (22) can be manipulated to give:

$$\frac{d\left(\ln(T_w - T_b)\right)}{dx} = -\frac{2\pi r_0 H}{\rho C_p Q} \tag{A1}$$

$$\frac{d\left(\ln(T_w - T_b)\right)}{dx} = -\frac{2H}{\rho C_p q} \tag{A2}$$

In the fully developed thermal region, where H is a constant, H (and $\mathrm{Nu} = HL/k$, with $L = 2r_0$ in the circular conduit geometry and $L = 4h$ in the sheet geometry) are thus related to the negative slopes (m) of linear fits to $\ln(T_w - T_b)$ versus x. Using T_b calculated from the full numerical solutions of (1) and (2), with $Q = \pi r_0^2 u_b$ and $q = 2hu_b$, negative slopes (m) of linear fits to $\ln(T_w - T_b)$ versus x were determined, and H and Nu were calculated from:

$$H = \frac{\rho C_p r_0 u_b}{2} m; Nu = \frac{r_0^2 u_b}{\kappa} m \tag{A3}$$

$$H = \rho C_p h u_b m; Nu = \frac{4h^2 u_b}{\kappa} m \tag{A4}$$

In the dissipation case, the thermally fully developed region is characterized by $dT_b/dx = 0$. Thus, H and Nu may be estimated by equating the terms on the right hand sides of (21) and (22). Siegel and Sparrow (1959) employed a similar approach to estimate Nusselt numbers for engineering heat transfer problems with arbitrary internal heat sources (e.g. heating elements) inside the conduit. We determined the bulk temperature in the thermally fully developed region ($T_{b\infty}$) by numerically integrating the temperature profiles obtained from numerical solutions of (1) and (2). Using these $T_{b\infty}$ values, we calculated H and Nu from:

$$H = \frac{\langle \Phi \rangle}{2\pi r_0 (T_{b\infty} - T_w)}; Nu = \frac{2r_0 H}{k} \tag{A5}$$

$$H = \frac{\langle \Phi \rangle}{2(T_{b\infty} - T_w)}; Nu = \frac{4hH}{k} \tag{A6}$$

It should also be noted that (A5, 6) are valid in the thermally fully developed region even if the wall temperature T_w is different from the fluid temperature T_0 at the entrance.

Acknowledgments

This research was funded by a NASA Earth and Space Science Fellowship (NESSF grant NNX14AL24H) and a Dissertation Completion Fellowship from the Department of Civil, Environmental, and Architectural Engineering at University of Colorado, Boulder. MATLAB scripts developed for this theoretical paper are available in a GitHub repository: https://github.com/aleahsommers/sommers_heat_transfer

References

Abe, H., & Antonia, R. A. (2016). Relationship between the energy dissipation function and the skin friction law in a turbulent channel flow. *Journal of Fluid Mechanics*, *798*, 140–164.

Bird, R. B., Stewart, W. E., & Lightfoot, E. N. (1960). Transport phenomena. 1960. *Madison, USA*.

Clarke, G. K. (2003). Hydraulics of subglacial outburst floods: new insights from the spring–hutter formulation. *Journal of Glaciology*, *49*(165), 299–313.

Creyts, T. T., & Clarke, G. K. (2010). Hydraulics of subglacial supercooling: theory and simulations for clear water flows. *Journal of Geophysical Research: Earth Surface*, *115*(F3).

Cuffey, K. M., & Paterson, W. S. B. (2010). *The physics of glaciers.* Academic Press.

Hewitt, I. (2013). Seasonal changes in ice sheet motion due to melt water lubrication. *Earth and Planetary Science Letters*, *371*, 16–25.

Hewitt, I., Schoof, C., & Werder, M. (2012). Flotation and free surface flow in a model for subglacial drainage. part 2. channel flow. *Journal of Fluid Mechanics*, *702*, 157–187.

Hewitt, I. J. (2011). Modelling distributed and channelized subglacial drainage: the spacing of channels. *Journal of Glaciology*, *57*(202), 302–314.

Hinze, J. (1975). Turbulence mcgraw-hill. *New York*, *218*.

Hoffman, M., & Price, S. (2014). Feedbacks between coupled subglacial hydrology and glacier dynamics. *Journal of Geophysical Research: Earth Surface*, *119*(3), 414–436.

Incropera, F. P., Lavine, A. S., Bergman, T. L., & DeWitt, D. P. (2007). Fundamentals of heat and mass transfer.

Kakaç, S., Shah, R. K., & Aung, W. (1987). Handbook of single-phase convective heat transfer.

Kays, W. M., & Crawford, M. E. (1993). *Convective heat and mass transfert* (No. BOOK). McGraw-Hill.

Kock, F., & Herwig, H. (2003). Dissipation in turbulent shear flows: a wall function approach for high reynolds numbers. *International Journal of Computational Fluid Dynamics*, *17*(5), 423–431.

Laadhari, F. (2007). Reynolds number effect on the dissipation function in wall-bounded flows. *Physics of Fluids*, *19*(3), 038101.

Lawn, C. (1971). The determination of the rate of dissipation in turbulent pipe flow. *Journal of Fluid Mechanics*, *48*(3), 477–505.

Lee, M., & Moser, R. D. (2015). Direct numerical simulation of turbulent channel flow up to $\mathrm{re}_\tau \approx 5200$. *Journal of Fluid Mechanics*, *774*, 395–415.

London, A. L., & Shah, R. (1978). *Laminar flow forced convection in ducts: a source book for compact heat exchanger analytical data.* Academic Press.

Nye, J. (1976). Water flow in glaciers: jökulhlaups, tunnels and veins. *Journal of Glaciology*, *17*(76), 181–207.

Rotta, J. (1962). Turbulent boundary layers in incompressible flow. *Progress in aerospace sciences*, *2*(1), 1–95.

Spring, U., & Hutter, K. (1981). Numerical studies of jökulhlaups. *Cold Regions Science and Technology*, *4*(3), 227–244.

Taylor, G. I. (1935). Statistical theory of turbulence. *Proceedings of the Royal Society of London. Series A, Mathematical and Physical Sciences*, *151*(873), 421–444.

Walder, J. S. (1982). Stability of sheet flow of water beneath temperate glaciers and implications for glacier surging. *Journal of Glaciology*, *28*(99), 273–293.

Walder, J. S. (1986). Hydraulics of subglacial cavities. *Journal of Glaciology*, *32*(112), 439–445.

Wasan, D., Tien, C., & Wilke, C. (1963). Theoretical correlation of velocity and eddy viscosity for flow close to a pipe wall. *AIChE Journal*, *9*(4), 567–569.

Werder, M. A., Hewitt, I. J., Schoof, C. G., & Flowers, G. E. (2013). Modeling channelized and distributed subglacial drainage in two dimensions. *Journal of Geophysical Research: Earth Surface*, *118*(4), 2140–2158.

Zanoun, E.-S., Durst, F., & Nagib, H. (2003). Evaluating the law of the wall in two-dimensional fully developed turbulent channel flows. *Physics of Fluids*, *15*(10), 3079–3089.

Zanoun, E.-S., Nagib, H., & Durst, F. (2009). Refined cf relation for turbulent channels and consequences for high-re experiments. *Fluid dynamics research*, *41*(2), 021405.